Electronic energy band parameters of CuInSe₂: Landau levels in magnetotransmission spectra

M. V. Yakushev [1,2,3,4,*] A. V. Rodina,[5] R. P. Seisyan,[5] Yu. E. Kitaev,[5] S. A. Vaganov,[5] M. A. Abdullaev,[6] A. V. Mudryi,[7] T. V. Kuznetsova,[1,3] C. Faugeras,[8] and R. W. Martin[2]

[1]*M.N. Miheev Institute of Metal Physics of UB RAS, 18 S. Kovalevskaya Street, 620108 Ekaterinburg, Russia*
[2]*Department of Physics, SUPA, Strathclyde University, G4 0NG Glasgow, United Kingdom*
[3]*Ural Federal University, Ekaterinburg 620002, Russia*
[4]*Institute of Solid State Chemistry of the UB RAS, Ekaterinburg 620990, Russia*
[5]*Ioffe Institute, St. Petersburg 194021, Russia*
[6]*Institute of Physics of the Russian Academy of Sciences, Makhachkala 367000, Russia*
[7]*Scientific-Practical Material Research Centre of the National Academy of Sciences of Belarus, 19 P. Brovki, Minsk 220072, Belarus*
[8]*LNCMI, 25 avenue des Martyrs, BP 166, 38042 Grenoble Cedex 9, France*

Magnetotransmission (MT) at magnetic fields up to 29 T was used to study the electronic structure of CuInSe₂ in thin polycrystalline films. The zero field absorption spectra exhibited resolved *A*, *B*, and *C* free excitons. Quantum oscillations, due to diamagnetic excitons comprising electrons and holes from Landau levels quantized in the conduction and valence band, respectively, appeared in the MT spectra at fields over 5 T. Spectral energies of Landau levels and binding energies of the corresponding diamagnetic excitons, theoretically calculated assuming a quasicubic approximation of the CuInSe₂ tetragonal lattice structure, helped to identify the character of the experimentally observed diamagnetic excitons. Spectral energies of diamagnetic excitons in the MT spectra with different circular polarizations were used to determine the electron and light hole effective masses, whereas heavy hole masses as well as the γ and γ_1 Luttinger parameters, E_p Kane energy, and F parameter of the influence of remote bands, as well as their polaron values, were calculated using the Luttinger theory.

I. INTRODUCTION

A direct bandgap (E_g) of 1 eV as well as a high absorption coefficient make the semiconductor CuInSe₂ a suitable material for the absorber layer of solar cells [1]. A record solar conversion efficiency of 23.3% [2] achieved for such cells with Cu(In, Ga)Se₂-based absorbers (gallium is added to match the absorption with the solar spectrum) and the excellent stability of these cells help position them as leading contenders for thin film photovoltaic (PV) devices. However, the electronic properties of CuInSe₂ are much less understood than those of Si or binary semiconductors. This lack of knowledge results in the significant gap between the achieved performance records and a theoretical efficiency limit of 30% for single junction PV devices [3]. Improvements in the level of knowledge of CuInSe₂, in general, and of the fundamental electronic properties in particular would help to accelerate the solar cell development process and reduce this gap.

The alternation of indium and copper atoms on the cation sublattice of CuInSe₂ generates a small and negative tetragonal distortion τ ($\tau = 1 - c/2a$, where c and a are the lattice constants) of -0.5%, which splits the valence band into the *A*, *B*, and *C* subbands [1]. Following a quasicubic model [4] this splitting can be interpreted as the simultaneous influence of the spin-orbit Δ_{so} and crystal-field Δ_{cf} couplings. In high structural quality CuInSe₂ single crystals these couplings have values of 234.7 and 5.3 meV, respectively [5].

Magneto-optical spectroscopy is an efficient tool to study the electronic properties of semiconductors [6]. However, this technique achieves the best outcomes when concentrations of defects are low, which promotes the resolution of clear excitonic features in the optical spectra. Weak magnetic field data have been used to analyze excited states of the *A* and *B* free excitons, allowing determination of their binding energies [7], *g* factors, hole effective masses, and their anisotropy [8]. The use of strong magnetic fields has allowed demonstration of fans of Landau levels in absorption spectra of thin polycrystalline films of CuInSe₂ [9], which exhibited resolved *A* and *B* excitons at zero field [10]. Such fans appear due to the excitation of electrons and holes from Landau levels in the conduction and valence band, respectively [11]. Analysis of the *C* exciton fan allowed determination of the binding energy for this exciton, E_g as well as the hole effective mass for the *C* valence subband [9]. Analysis of the Landau level fans, related to the *A* and *B* excitons, would provide an opportunity to calculate a self-consistent set of *kp*–theory parameters for the electronic structure of CuInSe₂. As well as improving the general level of understanding of CuInSe₂ these band parameters are also important for technologists developing solar cells based on this material. The achievement of high efficiency devices is aided by increasing the mobility of the carriers, for which an understanding of effective masses is important. Furthermore the anisotropy of the masses can indicate

---

*michael.yakushev@strath.ac.uk

an optimal crystallographic orientation of the absorber along which the mobility can be increased due to reduced masses for the carriers. The electron masses are most significant as they determine the mobility of electrons in the space charge region of the *p*-type absorption layer. The dependence of the masses on band-filling is also technologically important making it useful to gain understanding of the nonparabolicity.

This study uses analysis of Landau fans in the magnetotransmission (MT) spectra of thin polycrystalline films of CuInSe$_2$ to determine the electron and hole effective masses, the Luttinger and Kane parameters, as well as their polaron values.

II. EXPERIMENTAL DETAILS

Polycrystalline films of CuInSe$_2$ with a thickness of 1.5 μm and near stoichiometric [Cu]/[In] and [Cu+In]/[Se] ratios (determined to be 1.01 and 1.00, respectively, by energy dispersive x-ray analysis) were fabricated on glass substrates by the selenization of thermally evaporated Cu and In [10]. The surface morphology of these films was examined by scanning electron microscopy (SEM) using an S-806 (Hitachi, Japan) microscope at an electron beam energy of 20 keV. The structural properties and presence of secondary phases of the films were studied by x-ray diffraction (XRD) using a Brucker D8 ADVANCE diffractometer.

MT measurements of the films were carried out at 4.2 K in a helium vapor cryostat placed in the bore of a 20-MW resistive magnet, providing magnetic fields *B* up to 29 T, in the Faraday configuration. The light beam from a 100-W tungsten halogen lamp was delivered to the film under examination using optical fibers. The transmitted light was then passed to the slits of a 0.3 m monochromator also using optical fibers. The dispersed signal was registered using a liquid nitrogen cooled InGaAs array detector. A linear polarizer and a quarter-wave plate were used for circular polarization resolved measurements. The intensity of the MT spectra *I(B)* was normalized using the zero-field spectrum *I*(0T). The spectral position of the lines was measured with an accuracy of 0.1 meV at a spectral resolution of 0.2 meV.

III. RESULTS AND DISCUSSION

Plan view and cross section SEM micrographs, shown in Figs. 1(a) and 1(b), respectively, demonstrate homogeneous films with densely packed grains with sizes varying from 0.4 to 0.8 μm. The x-ray diffraction pattern, shown in Fig. 1(c), reveals the chalcopyrite structure with a (112) preferential orientation of the grains. The lattice parameters are calculated to be $a = 0.578$ nm and $c = 1.162$ nm, giving a tetragonal distortion of $\tau = -0.43\%$.

Room temperature Hall effect measurements showed the *n*-type conductivity of the films, an electron density of 4×10^{16} cm^{-3} and mobility of 15 cm^2/V s.

The zero magnetic field absorption spectrum is shown in Fig. 2(a) and reveals *A* and *B* excitons at 1.0413 and 1.0444, respectively.

A wide range spectrum exhibiting the *A*, *B*, and *C* excitons is shown in Fig. 2(b). The bandgap energies of $E_{gA} = 1.0498$ eV, $E_{gB} = 1.0528$ eV and $E_{gC} = 1.2828$ eV were cal-
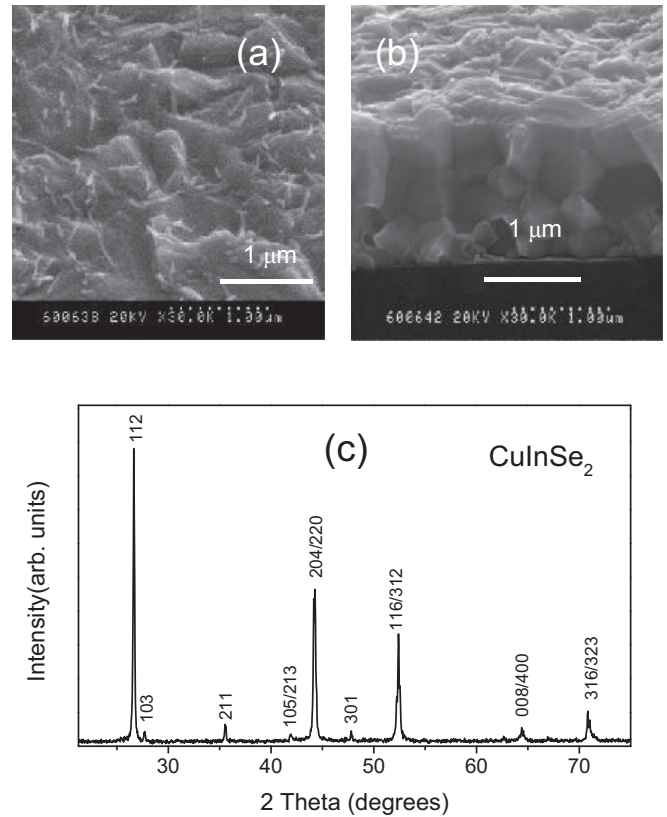

FIG. 1. SEM micrographs of the CuInSe$_2$ films: plan view (a) and cross section (b). XRD pattern (c).

culated assuming binding energies of the *A*, *B*, and *C* excitons of 8.5, 8.4, and 8.5 meV, respectively [7,9]. An evolution of the normalized, unpolarized MT spectra *I(B)/I*(0T) with increasing *B* is shown in Fig. 3(a). The *A* and *B* exciton ground states dominate the spectra. Their spectral positions correspond to the minima of the grey scale density. The spectral position of the features, appearing in the spectra near the *A*, *B*, and *C* excitons at fields exceeding 5 T, show a linear dependence on B. This demonstrates achievement of the strong field limit at which the magnetic field forces exceed
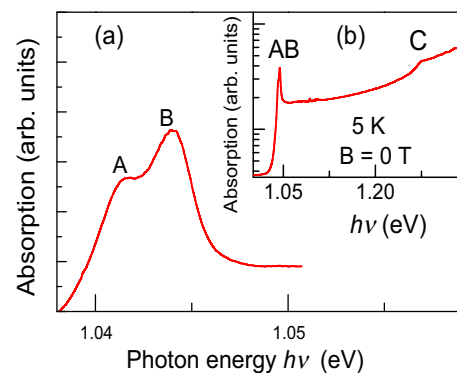

FIG. 2. The *A* and *B* excitons in an absorption spectrum of CuInSe$_2$ thin films plotted on a linear scale (a). The inset shows a wider plot with *A*, *B*, and *C* excitons in the zero-field absorption spectrum plotted on a logarithmic scale (b).
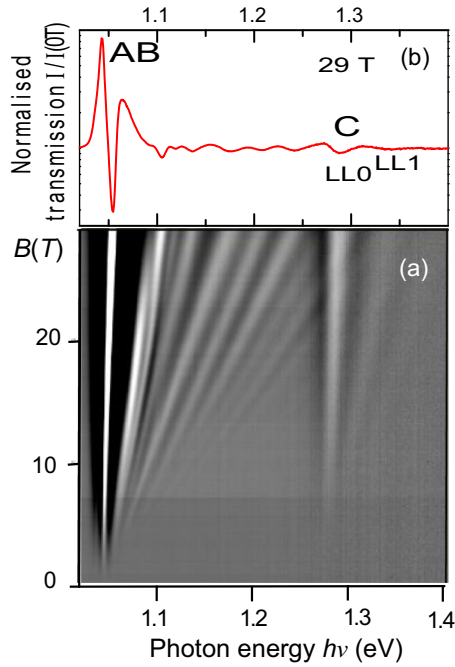
FIG. 3. The evolution of normalized MT spectra with magnetic field B (showing Landau fans) measured using nonpolarized light (a), the higher the normalized intensity $I(B)/I(0T)$ the lighter is the grey scale density. A normalized MT spectrum measured at 29 T (b).

the Coulomb forces resulting in Landau quantization of the circular motion of charge carriers in the plane perpendicular to B. Oscillations of $I(B)/I(0T)$, associated with Landau levels [11], can also be seen in the MT spectrum measured at 29 T shown in Fig. 2(b). The spectral region of the A and B excitons shows clear Landau fans.

The strong field limit can be estimated by the modified Elliott-Loudon criterion $n^2(a_{exc}/L)^2 \gg 1$, where n is the principal quantum number, a_{exc} is the exciton radius, and $L = \sqrt{c\hbar/eB}$ is the magnetic length [11]. For the CuInSe$_2$ ground state ($n = 1$) this limit can be achieved at B of 30 T [9]. However, for the first excited state ($n = 2$) the strong field limit is reached just above 5 T as can be seen experimentally in the MT spectra in Fig. 3(a), where Landau level fans with spectral energies linearly dependent on B become clearly apparent.

The symmetry of CuInSe$_2$ is described by the space group $D_{2d}^{12}(I\bar{4}2d)$ (No. 122) with a body-centered-tetragonal lattice [12]. The primitive unit cell of such a lattice contains two formula units whereas the crystallographic unit contains four such units as shown in Fig. 4(a). The atomic arrangement for this symmetry (occupied Wyckoff positions) is shown in the upper part of Table I.

Deviations of the lattice symmetry from the cubic one result in a drastic increase of the number of parameters required for calculations of the band structure. Therefore, it is convenient to use a model representing noncubic lattices with small deviations from the cubic structure as quasicubic ones.

A quasicubic model, where crystal field induced splitting of the valence band of hexagonal binary semiconductors, was described as a result of uniaxial deformations [13], was
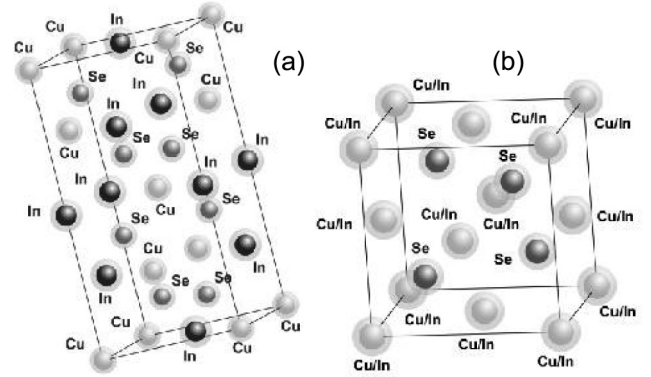

FIG. 4. Chalcopyrite lattice structure of CuInSe$_2$ (a), quasicubic approximation of the lattice structure of CuInSe$_2$ by the randomization of the Cu and In atoms positions on the cation sublattice (b).

successfully adopted to analyse Landau levels in MT spectra of the CdSe hexagonal structure [14]. Another quasicubic model was recently developed for theoretical analysis of the electronic structure of CuInS$_2$, a compound isostructural to CuInSe$_2$ and with $\tau = -0.8\%$ [1], by randomization of Cu and In atoms on the cation sublattice [15]. Following this model we approximated the tetragonal lattice of CuInSe$_2$ by a quasicubic one making the c lattice constant (along the tetragonal z axis) equal to the doubled a (along x and y axes). As a result, the tetragonal unit cell transforms into two inequivalent cubic (within an accuracy of 0.43%) unit cells. The Cu and In atoms are then substituted by a virtual Cu/In atom and Se is shifted by about 8% along the x axis to the cube diagonal.

After this the body-centered-tetragonal unit cell of CuInSe$_2$ transforms into two identical face-centered-cubic cells reducing the tetragonal lattice symmetry to an approximately cubic one.

The symmetry of such a cubic structure is described by the space group $O_h^7(F\bar{4}3m)$ (No. 216), with Cu/In and Se atoms occupying the Wyckoff positions in the unit cell of the cubic lattice given in the lower part of Table I. The unit cells of body-centered-tetragonal and face-centered–cubic lattices, shown in Figs. 4(a) and 4(b), are drawn using the

TABLE I. Exact and approximate symmetries of CuInSe$_2$: body-centered-tetragonal and face-centered-cubic lattice, respectively.

Tetragonal lattice/Atoms	Cu	In	Se
Exact Wyckoff position	2a	2b	4d
Exact site symmetry	$\bar{4}$	$\bar{4}$	2
x	0	0	0.2293
y	0	0	0.5000
z	0	0.5	0.1250
Quasicubic lattice/Atoms	Cu/In		Se
Approximate Wyckoff position	1a		1c
Approximate site symmetry	$\bar{4}3m$		$\bar{4}3m$
x	0		0.25
y	0		0.25
z	0		0.25

VISUALIZE code of the Bilbao Crystallographic Server [16]. Similar approximate symmetry approaches have been proved to be efficient for analysis of lattice vibrations explaining the presence of line doublets and changes of relative intensity of allowed spectral lines in phonon spectra [17–19].

In further analysis $CuInSe_2$ is considered as a quasicubic semiconductor with a bandgap of $E_g = [E_g(B) + E_g(A)]/2 = 1.05195 \, \text{eV}$ and a spin orbital splitting $\Delta_{so} = E_g(C) - E_g = 231.5 \, \text{meV}$. The condition $\Delta_{so} \gg \Delta_{AB}$, where $\Delta_{AB} = E_g(B) - E_g(A) = 3.0 \, \text{meV}$ is the crystal field induced splitting of the topmost valence band, allows determination of the crystal field parameter in the quasicubic model as $\Delta_{cr} = 3\Delta_{AB}/2 = 4.5 \, \text{meV}$ [14]. The spectral energies of Landau levels can be calculated using the Pidgeon-Brown determinant equation [20] in the Aggarwal form [21] assuming shear deformation. To analyze the effects of strong magnetic fields we first consider the motion of electrons and holes in the plane perpendicular to the magnetic field. Quantization of this motion results in the formation of Landau levels [11]. Then we take into account the Coulomb interaction between electrons and holes, which results in the formation of an infinite series of one-dimensional states of diamagnetic excitons corresponding to each Landau level [11]. The energies of Landau levels for electrons $E_n^\pm$ for $\boldsymbol{B}$ along z can be found as follows:

$$E_n^\pm = \hbar\omega_0 \left[\frac{m_0}{m_e(\epsilon)}(n + 1/2) \pm \frac{1}{4}g_e \right], \qquad (1)$$

where $\hbar\omega_0 = 2\mu_B B$ is the electron cyclotron energy (μ_B is the Bohr magneton and m_0 is the free electron mass), $m_e(\epsilon)$ is the electron effective mass at ϵ, the energy from the bottom of the conduction band, n is the Landau level number for electrons ($n = 0, 1, 2\ldots$), $\pm$ indicates the electron spin projection $s = \pm 1/2$ on the magnetic field direction $\boldsymbol{B}$, and g_e is the electron effective Lande factor.

We neglect the dependence of g_e on ϵ and consider $m_e(\epsilon)$ as [22]

$$\frac{m_0}{m_e(\epsilon)} = 1 + 2F + \frac{E_p}{3}\left[\frac{2}{E_g + \epsilon} + \frac{1}{E_g + \Delta_{so} + \epsilon}\right], \qquad (2)$$

where $2F$ is the contribution of remote bands and $E_p = 2m_0 P^2/\hbar^2$ is the Kane energy parameter, whereas P is the Kane matrix element of the momentum operator, describing the conduction and valence band coupling, $P = i\hbar\langle S|\hat{p}_z|\rangle/m_0$.

The energies $E_{l,\lambda}$ of Landau levels for holes from the topmost valence band can be found as

$$E_{l,\lambda} = \hbar\omega_0 \left[\frac{\alpha_{l,\lambda} + \alpha_{l,\lambda_1}}{2} + \left(\frac{5}{4} - \lambda^2\right) \right.$$
$$\left. \times \sqrt{3l(l + \lambda + \lambda_1)\gamma^2 + \frac{(\alpha_{l,\lambda} - \alpha_{l,\lambda_1})^2}{4}} \right], \qquad (3)$$

where l is the Landau level number for holes involved in the formation of diamagnetic excitons. Each of these hole states comprises two states from the top of the valence band (mixed by the magnetic field) with their spin indexes λ and λ_1 differing by 2. Heavy holes with their momentum projection on $\boldsymbol{B}$ $\lambda = \pm 3/2$ also admix states with $\lambda_1 = 4\lambda(\lambda^2 - 5/2)/3 =$

$\mp 1/2$, whereas light holes with projections $\lambda = \pm 1/2$ also admix states with $\lambda_1 = \mp 3/2$. The $\alpha_{l,\lambda}$ coefficient is given by

$$\alpha_{l,\lambda} = \gamma_1 l - (5/4 - \lambda^2)(l + \lambda)\gamma + \lambda(\gamma_1 - \kappa) + \delta(5/4 - \lambda^2), \qquad (4)$$

where $\delta = \Delta_{AB}/\hbar\omega_0$, γ_1 and $\gamma = \gamma_2 = \gamma_3$ are effective mass Luttinger parameters and κ is the magnetic one [22].

Spectral energies of the optically allowed diamagnetic excitonic transitions can be calculated theoretically as [11]

$$E_{n,M,\lambda}^\pm = E_g + E_n^\pm + E_{l,\lambda} - R_{n,M,\lambda}, \qquad (5)$$

where $R_{n,M,\lambda}$ are binding energies of diamagnetic excitons formed for the Landau level with electron number n and hole number $l = n - M + \frac{1}{2}$, where $M = \pm 1/2, \pm 3/2$ is the projection of the hole (belonging to this diamagnetic exciton) total angular momentum on $\boldsymbol{B}$. Note that M can be either equal to λ or λ_1. $R_{n,M,\lambda}$ can be calculated by solving the Schrodinger equation (with the Hamiltonian, describing relative motion of the electron and hole perpendicular to the magnetic field) within the adiabatic approximation. Such an equation was solved in Ref. [23] for cubic semiconductors assuming isotropic effective mass of the electron $m_e = m_e(0)$. However, in order to find the exciton energies from Eq. (5) we require parameters of the electronic band structure. Some of them, namely E_g, Δ_{cf}, and Δ_{so}, are determined experimentally in this paper. For m_e/m_0 and m_{so}/m_0 we used experimental values of 0.09 ± 0.01 [24] and 0.31 ± 0.12 [9], respectively. An absolute value of 1.27 for the effective g factor of the A free exciton g_{ex} was determined in Ref. [8] analyzing low field Zeeman splitting at $\boldsymbol{B} \perp z$ and assuming an isotropic low frequency dielectric constant ε calculated as the average value $\varepsilon = (\varepsilon^{||} \cdot \varepsilon^{\perp 2})^{1/3}$ of the theoretically calculated anisotropic values of $\varepsilon^\perp = 11.0$ and $\varepsilon^{||} = 10.3$ [26]. In general, g_{ex} combines the electron g_e and hole g_h components $|g_{ex}| = |g_e \pm g_h|$. However, at $\boldsymbol{B} \perp z$ the hole component becomes vanishing small. Therefore, for isotropic g_e we can take its modulus of 1.27. Calculations were performed for both polarizations, left (σ^+) and right circular polarizations (σ^-). Note, that the transitions with $M = +3/2$ and $s = -1/2$ as well as $M = +1/2$ and $s = +1/2$ can be observed for the σ^+ polarization, whereas $M = -3/2$, $s = +1/2$ and $M = -1/2$, $s = -1/2$ for σ^-. This allows us to determine the sign of g_e, as only $g_e = -1.27$ resulted in a good match of the calculated Landau level energies and the experimental MT spectra.

However, at this stage we do not know γ_1, E_p, F, γ and κ. At first a preliminary estimate of γ_1 was calculated as proposed in Ref. [14]: using the average of experimental binding energies for the A and B excitons [7] as an effective Rydberg and assuming the polaron reduced mass μ_p determined as $1/\mu_p = 1/m_{ep} + \gamma_1$, where m_{ep} is the polaron effective electron mass of $m_{ep}/m_0 = 0.093$ [7]. Preliminary E_p and F were then calculated making sure that values of m_{so} and m_e, determined in further calculations, were matching their experimental values of $m_{so}/m_0 = 0.31$ [9] and $m_e/m_0 = 0.09$ [24], respectively. Preliminary estimates of the parameters $E_p = 13.9 \, \text{eV}$, $F = 1.16$, $\gamma_1 = 3.22$, $\gamma = 1.0$, and $\kappa = 0$ were used to calculate theoretical spectra which were then used to identify the character of the lines in the experimental MR spectra.
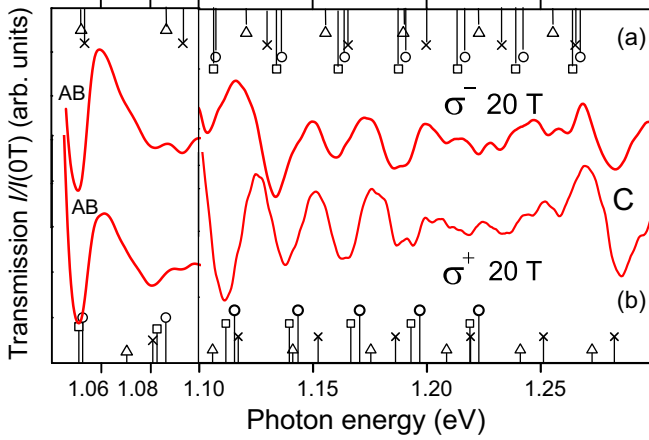
FIG. 5. MT spectra measured at 20 T for σ^- (a) and σ^+ (b) polarizations (solid lines). The symbols show calculated energies of diamagnetic excitons comprising an electron (from level n) and holes from level $l = n - M + \frac{1}{2}$, with $M = \pm 1/2, \pm 3/2$ (upper sign "+" for σ^+ and lower sign "−" for σ^- spectra), $\lambda = \pm 3/2$ for the heavy hole ($\square$ and $\circ$), and $\lambda = \pm 1/2$ for the light hole ($\triangle$ and x), respectively.

Experimental MT spectra of CuInSe2 at 20 T for σ^- and σ^+ polarizations of the light beam are shown by solid lines in Figs. 5(a) and 5(b), respectively.

The symbols with drop lines show theoretically calculated spectral positions of the diamagnetic excitons determined by solving Eq. (5) and after subtracting corresponding binding energies $R_{n,M,\lambda}$ from the energies of Landau levels. For heavy holes (symbols $\square$ and $\circ$) $\lambda = \pm 3/2$, whereas, for light holes (symbols $\triangle$ and x) $\lambda = \pm 1/2$. The length of the lines is arbitrary. Figures 5(a) and 5(b) demonstrate a good match of the theoretical spectral positions with the minima of $I(B)/I(0)$ in the experimental MT spectra suggesting that these preliminary parameters can be used to identify the character of the excitons. To determine m_e and its nonparabolicity we identified two excitons, present in the MT spectra with opposite circular polarizations, comprising the same hole with the Landau level number l and two electrons with the same s: one electron from Landau level with number $n + 1$ and the other with $n - 1$. Thus, due to selection rules their M values differ by 2 and they were identified in the spectra with opposite circular polarizations. The energy difference $(E_{n+1}^\pm - E_{n-1}^\pm)$ between such excitons is related to m_e and the nonparabolicity α_p as follows:

$$\frac{E_{n+1}^\pm - E_{n-1}^\pm}{2\hbar\omega_0} = \frac{m_0}{m_e} - p_c(2n+1)\hbar\omega_0, \quad n = 1, 2 \ldots, \tag{6}$$

where

$$\frac{m_0}{m_e(\epsilon)} = \frac{m_0}{m_e} - \alpha_p\epsilon \quad \text{and} \quad p_c = \frac{m_0}{m_e}\alpha_p. \tag{7}$$

To reduce the statistical errors, generated by the scatter of the experimental data points, we used the arithmetic average of the energy differences $(E_{n+1}^\pm - E_{n-1}^\pm)$, calculated for two series of excitons for 15 and 20 T. The dependence of such an
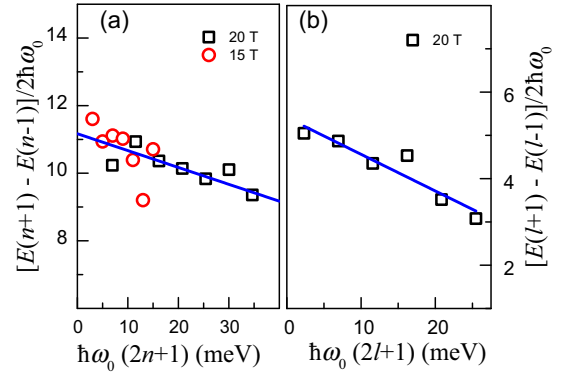

FIG. 6. The relative difference of the spectral energies of two excitons, comprising a hole (with number l) and two different electrons, with Landau level numbers $n + 1$ and $n - 1$ for magnetic fields of 15 and 20 T plotted on a $\hbar\omega_0(2n + 1)$ scale (c). The relative difference of the spectral energies of two excitons, comprising an electron (with number n) and two different holes, with Landau level numbers $l - 1$ and $l + 1$, for magnetic fields of 20 T plotted on a $\hbar\omega_0(2l + 1)$ scale (d).

average for the two magnetic fields along with the best linear fit through the experimental points are shown in Fig. 6(a). The intercept of the fitted line represents the inverse electron mass m_0/m_e, which determines $m_e/m_0 = 0.090 \pm 0.002$ at $\epsilon = 0$. The slope p_c of the line in Fig. 6(a) was used to calculate $\alpha_p = (0.0045 \pm 0.014)\,\text{eV}^{-1}$. Its value is also shown in Table II. Expanding $\frac{m_0}{m_e(\epsilon)}$ given by Eq. (2) in a Taylor series for small ϵ enables the relation between nonparabolicity parameter α_p and the Kane energy parameter E_p to be obtained as [25]

$$\alpha_p = E_p\left[2/E_g^2 + 1/(E_g + \Delta_{so})\right]/3, \tag{8}$$

giving $E_p = (5.55 \pm 0.04)\,\text{eV}$. This value is close to $E_p = 7.95\,\text{eV}$, determined in Ref. [15] for CuInS2. $F = 2.61 \pm 0.03$ was determined at $\epsilon = 0$ from Eq. (2) assuming that the nonparabolicity of m_e is entirely due to the valence band contribution. Thus, using the determined values of E_p, m_{so}, E_g, and Δ_{so} we calculated $\gamma_1 = 3.5 \pm 1.3$ as follows [14]:

$$\gamma_1 = \frac{1}{m_{so}} + \frac{E_p}{3}\left[\frac{1}{E_g} - \frac{1}{E_g + \Delta_{so}}\right]. \tag{9}$$

Theoretical studies [26] suggested a rather weak anisotropy of the conduction band with the difference of the electron mass perpendicular and parallel to the optical axis c of 10%. Therefore, we expect the determined electron masses m_e to be accurate within 10%, although their statistical error of $0.002\,m_0$ is much smaller. The band structure parameters α_p, E_p, and F, calculated using m_e, should also be weakly dependent on the orientation of the crystallites in the films. Their statistical errors are rather small. Increasing the error of

TABLE II. The determined band parameters.

Band parameters	γ_1	γ	m_e/m_0	E_p (eV)	F	α_p (eV^{-1})
Values	3.5	0.95	0.090	5.55	2.61	0.0045

TABLE III. Bare and polaron effective masses of the *A* and *B* valence band holes, m_A and m_B, respectively.

Masses	m_e/m_0	$m_{A\parallel}/m_0$	$m_{A\perp}/m_0$	$m_{B\parallel}/m_0$	$m_{B\perp}/m_0$
Bare	0.090	0.6	0.22	0.19	0.39
Polaron	0.093	0.7	0.24	0.20	0.41
Theory [24]	0.083	0.7	0.14	0.12	0.25

m_e to $0.01m_0$ does not influence the error of α_p and E_p whereas that of F increases significantly $F = 2.6 \pm 1.3$.

Once the oscillator character of excitons in the MT spectra is identified we determined effective masses of the heavy and light holes by analyzing the dependence of the spectral energy difference between two excitons comprising electrons from the same electron level n and two different heavy or light holes with Landau level numbers $l - 1$ and $l + 1$. Such excitons with the *M* difference of 2 were identified in the spectra with opposite circular polarizations. The lowest level of scatter of the experimental data for the light hole Landau levels with $\lambda = \pm 1/2$ was found for MT spectra at 20 T. These data along with the best linear fit, plotted on a $\hbar\omega_0(2l + 1)$ scale, are shown in Fig. 6(b). The intercept of the fitted line determines the inverse light hole mass, related to the Luttinger parameters in a model cubic semiconductor with $\delta = 0$, as [27] $m_0/m_{lh} = (\gamma_1 + 2\gamma)$ and results in the light hole mass $m_{lh}/m_0 = 0.185 \pm 0.008$. It provides us with an opportunity to calculate the effective Luttinger parameter $\gamma = 0.95 \pm 0.75$ using the following expression $\gamma = (m_0/m_{lh} - \gamma_1)/2$ [27]. This value is also shown in Table II. Heavy hole masses, determined using similar analysis for the Landau levels with $\lambda = \pm 3/2$, exhibited a significant scatter of the data making them unreliable. Therefore instead we used γ_1 and γ to calculate the parallel $m_{h\parallel}$ and perpendicular $m_{h\perp}$ components of anisotropic effective bare hole masses for the *A* and *B* valence subbands [27]. Under the condition $\Delta_{so} \gg \Delta_{cr}$ these masses can be calculated as follows [14]:

$$m_{A\parallel}/m_0 = 1/(\gamma_1 - 2\gamma), \tag{10}$$

$$m_{A\perp}/m_0 = 1/(\gamma_1 + \gamma), \tag{11}$$

$$m_{B\parallel}/m_0 = 1/(\gamma_1 + 2\gamma), \tag{12}$$

$$m_{B\perp}/m_0 = 1/(\gamma_1 - \gamma). \tag{13}$$

These calculations resulted in values of $m_{A\parallel}/m_0 = 0.6 \pm 1.1$, $m_{A\perp}/m_0 = 0.22 \pm 0.10$, $m_{B\parallel}/m_0 = 0.19 \pm 0.10$ and $m_{B\perp}/m_0 = 0.39 \pm 0.31$, respectively. The determined values are collected in Table III. The density of state (DOS) bare hole masses of $m_{ADOS}/m_0 = 0.31 \pm 0.27$ and $m_{BDOS}/m_0 = 0.30 \pm 0.21$ were calculated using the expression $m_{hDOS}^* = (m_{h\parallel} m_{h\perp}^2)^{1/3}$ for the *A* and *B* valence subbands, respectively. The determined masses are also collected in Table III. A rather high error of 37% of the γ_1 Luttinger parameter is produced by that of the *C* valence subband hole mass which is assumed to be isotropic [8]. Unlike its conduction band the valence band of CuInSe$_2$ exhibits significant anisotropy as has been predicted theoretically [24]

and confirmed experimentally [8]. Therefore, the light hole mass, determined in our paper for the polycrystalline films, as well as the γ Luttinger parameter, calculated using this mass, should be considered as estimates. The errors calculated for the hole masses of the *A* and *B* valence subbands are also high and only estimates.

The electron mass m_e, found from the fit in Fig. 6(a), retained its preliminary value suggesting that another iteration is not necessary. The contribution to the nonparabolicity due to the valence band of m_e, estimated as $m_0/m_e - 2F = 5.98$, is close to that due to remote bands, estimated as $2F = 5.22$ suggesting that our $E_p = 5.55$ eV may be underestimated [27]. However, at this stage we do not take this possibility into account.

Polaron electron $m_{ep} = m_e(1 + \alpha_{Fe}/6)$ and hole $m_{hp} = m_h(1 + \alpha_{Fh}/6)$ effective masses are heavier than the bare ones due to the interaction of the carriers with optical phonons in polar lattices.

An isotropic Fröhlich coupling constant for the electron $\alpha_{Fe} = \sqrt{m_e e^4 / 2\hbar^2 \varepsilon^{*2} E_{lo}} = 0.202$, calculated in Ref. [8] for a longitudinal optical phonon energy E_{lo} of 29 meV [28], and a high-frequency dielectric constant [26] ε^*, determined as $\frac{1}{\varepsilon^*} = \frac{1}{\varepsilon_\infty} - \frac{1}{\varepsilon}$, where $\varepsilon_\infty = (\varepsilon_\infty^\parallel \times \varepsilon_\infty^{\perp 2})^{1/3}$, whereas the anisotropic high-frequency dielectric constants $\varepsilon_\infty^\parallel = 7.8$ and $\varepsilon_\infty^\perp = 8.2$ were theoretically calculated in Ref. [26]. This Fröhlich coupling constant was used in Ref. [8] to determine the polaron electron effective mass $m_{ep} = 0.093m_0$.

Following Ref. [29], we calculated an isotropic Fröhlich coupling constant for holes $\alpha_{Fh} = \alpha_{Fe}/\sqrt{m_e \gamma_1} = 0.36$ and renormalized the effective Luttinger parameters as $\gamma_p = \gamma/(1 + \alpha_{Fh}/6) = 0.9$ and $\gamma_{1p} = \gamma_1/(1 + \alpha_{Fh}/6) = 3.3$. The polaron effective hole masses calculated with renormalized Luttinger parameters are shown in Table III. The DOS polaron hole effective masses of $m_{ADOSp}/m_0 = 0.33m_0$ and $m_{BDOSp}/m_0 = 0.32m_0$ were calculated for the *A* and *B* valence subbands, respectively. There is good agreement for $m_{A\parallel}$ whereas theoretical $m_{A\perp}$ is significantly smaller than that determined in this study. The anisotropy of the *A* subband hole of 5.5 [8], determined from low field magneto-photoluminescence experiments on high structural quality oriented single crystals of CuInSe$_2$, calculated as the ratio $m_{A\parallel}/m_{A\perp}$, is greater than our experimental value of 2.7. This can be attributed to the scatter of the grain orientation reducing the anisotropy in the studied films. Hole masses, theoretically calculated in Ref. [26], also shown in Table III, demonstrate, an agreement of the anisotropy character.

The polycrystalline nature of the material should also reduce the accuracy of the determined band structure parameters. Although the hole masses of the *A* and *B* valence subbands, determined from low field magneto-photoluminescence data [8], are greater than those determined in this study they are still within rather broad error bars.

To improve the accuracy of the MT measurements and that of the band parameters determined using magnetotransmission one should prepare oriented slabs of high quality single crystals of CuInSe$_2$ exhibiting the *A* and *B* free excitons in their PL and absorption spectra. However, the very high absorption coefficient of CuInSe$_2$ (of 5×10^5 cm^{-1} in the spectral range of the *A* and *B* free exciton) [10] requires such

slabs to be thinned to a micron. MT measurements on these single crystalline slabs, performed with the field, directed along the principal crystallographic axes, would reduce the scatter in the experimental data and allow more accurate band parameters to be determined.

IV. CONCLUSIONS

Landau fans were observed in MT spectra of thin polycrystalline CuInSe$_2$ films. These fans correspond to the recombination of diamagnetic excitons, constituting electrons from the conduction and holes from the valence A, B, and C subbands, quantized by strong magnetic fields. Spectral energies of Landau levels and diamagnetic exciton binding energies were theoretically calculated by representing the tetragonal lattice structure of CuInSe$_2$ as a quasicubic one under shear deformation. These calculations helped to identify the character of the transitions, observed in the MT spectra. Spectral energies of diamagnetic excitons from the MT spectra with opposite circular polarizations were used to determine the electron and light hole effective masses, whereas heavy hole masses as well as the γ and γ_1 Luttinger parameters, E_p Kane energy, and the F parameter of the influence of remote bands, as well as their polaron values were calculated using the Luttinger theory.

[1] J. L. Shay and J. H. Wernick, *Ternary Chalcopyrite Semiconductors - Growth, Electronic Properties, and Applications* (Pergamon, Oxford, 1975).

[2] M. A. Green, Y. Hishikawa, E. D. Dunlop, D. H. Levi, J. Hohl-Ebinger, M. Yoshita, and A. W. Y. Ho-Baillie, Prog. Photovolt. Res. Appl. **27**, 3 (2019).

[3] W. Shockley and H. J. Queisser, J. Appl. Phys. **32**, 510 (1961).

[4] J. E. Rowe and J. L. Shay, Phys. Rev. B **3**, 451 (1971).

[5] A. V. Mudriy, I. V. Bodnar, I. A. Viktorov, V. F. Gremenok, M. V. Yakushev, R. D. Tomlinson, A. E. Hill, and R. D. Pilkington, Appl. Phys. Lett. **77**, 2542 (2000).

[6] J. O. Dimmock and R. G. Wheeler, J. Appl. Phys. **32**, 2271 (1961).

[7] M. V. Yakushev, F. Luckert, C. Faugeras, A. V. Karotki, A. V. Mudriy, and R. W. Martin, Appl. Phys. Lett. **97**, 152110 (2010).

[8] M. V. Yakushev, F. Luckert, A. V. Rodina, C. Faugeras, A. V. Mudriy, A. V. Karotki, and R. W. Martin, Appl. Phys. Lett. **101**, 262101 (2012).

[9] M. V. Yakushev, A. V. Rodina, G. M. Shuchalin, R. P. Seisian, M. A. Abdullaev, A. Rockett, V. D. Zhivulko, A. V. Mudriy, C. Faugeras, and R. W. Martin, Appl. Phys. Lett. **105**, 142103 (2014).

[10] A. V. Mudryi, V. F. Gremenok, I. A. Victorov, V. B. Zalesski, F. V. Kurdesov, V. I. Kovalevski, M. V. Yakushev, and R. W.Martin, Thin Solid Films **431-432**, 193 (2003).

[11] R. P. Seisyan and B. P. Zakharchenya, in *Landau Level Spectroscopy*, edited by E. I. Rashba and G. Landwehr (North Holland, Amsterdam, 1991).

[12] S. Schor and G. Geandier, Cryst. Res. Technol. **41**, 450 (2006).

[13] J. J. Hopfield, J. Phys. Chem. Solids **15**, 97 *(1960)*.

[14] A. B. Kapustina, B. V. Petrov, A. V. Rodina, and R. P. Seysian, Phys. Solid State **42**, 1242 (2000).

[15] A. Shabaev, M. J. Mehl, and Al. L. Efros, Phys. Rev. B **92**, 035431 (2015).

[16] M. I. Aroyo, J. M. Perez-Mato, C. Capillas, E. Kroumova, S. Ivantchev, G. Madariaga, A. Kirov, and A. Wondratschek, Z. Kristallogr. **221**, 15 (2006).

[17] Yu. E. Kitaev, M. F. Limonov, A. G. Panfilov, R. A. Evarestovn, and A. P. Mirgorodsky, Phys. Rev. B. **49**, 9933 (1994).

[18] M. F. Limonov, E. A. Goodilin, X. Yao, S. Tajima, Y. Shiohara, and Yu. E. Kitaev, Phys. Rev. B **58**, 12368 (1998).

[19] Yu. E. Kitaev, M. I. Aroyo, and J. M. Perez-Mato, Phys. Rev. B **75**, 064110 (2007).

[20] C. R. Pidgeon and R. N. Brown, Phys. Rev. **146**, 575 (1966).

[21] R. L. Aggarwal, in *Semiconductors and Semimetals*, Vol. 9, edited by R. K. Willardson and A. C. Beer (Academic, New York, 1972), p. 151.

[22] E. O. Kane, J. Phys. Chem. Solids **1**, 249 (1956).

[23] S. I. Kokhanovskii, Yu. M. Makushenko, R. P. Seïsyan, Al. A. Efros, T. V. Yazeva, and M. A. Abdullaev, Fiz. Tverd. Tela (Leningrad) **33**, 1719 (1991) [Sov. Phys. Solid State **33**, 967 (1991)].

[24] H. Weinert, H. Neumann, H. Hobler, G. Kuhn, and N. V. Nam, Phys. Status Solidi B **81**, K59 (1977).

[25] A. V. Rodina and A.Yu. Alekseev, Phys. Rev. B **78**, 115304 (2008).

[26] C. Persson, Appl. Phys. Lett. **93**, 072106 (2008).

[27] J. M. Luttinger, Phys. Rev. **102**, 1030 (1956).

[28] H. Tanino, T. Maeda, H. Fujikake, H. Nakanishi, S. Endo, and T. Irie, Phys. Rev. B **45**, 13323 (1992).

[29] A. V. Rodina, M. Dietrich, A. Goldner, L. Eckey and A. Hoffmann, Al. L. Efros and M. Rosen, and B. K. Meyer, Phys. Rev. B **64**, 115204 (2001).